

SUBMITTED TO *ApJ* ON JULY 20, 2001; ACCEPTED ON OCTOBER 18, 2001.Preprint typeset using L<sup>A</sup>T<sub>E</sub>X style emulatej v. 14/09/00

## NUCLEAR CUSPS AND CORES IN EARLY-TYPE GALAXIES AS RELICS OF BINARY BLACK HOLE MERGERS

SWARA RAVINDRANATH<sup>1,2</sup>, LUIS C. HO<sup>1</sup>, AND ALEXEI V. FILIPPENKO<sup>2</sup>*Submitted to ApJ on July 20, 2001; accepted on October 18, 2001.*

## ABSTRACT

We present an analysis of the central cusp slopes and core parameters of early-type galaxies using a large database of surface brightness profiles obtained from *Hubble Space Telescope* observations. We examine the relation between the central cusp slopes, core parameters, and black hole masses in early-type galaxies, in light of two models that attempt to explain the formation of cores and density cusps via the dynamical influence of black holes. Contrary to the expectations from adiabatic-growth models, we find that the cusp slopes do not steepen with increasing black hole mass fraction. Moreover, a comparison of kinematic black hole mass measurements with the masses predicted by the adiabatic models shows that they overpredict the masses by a factor of  $\sim 3$ . Simulations involving binary black hole mergers predict that both the size of the core and the central mass deficit correlate with the final black hole mass. These relations are qualitatively supported by the present data.

*Subject headings:* black hole physics — galaxies: elliptical and lenticular, cD — galaxies: fundamental parameters — galaxies: structure

## 1. INTRODUCTION

High-resolution images obtained using ground-based and *Hubble Space Telescope* (HST) observations have shown that density cusps are ubiquitous in the centers of early-type galaxies and true constant-density cores are extremely rare (Kormendy 1985; Lauer 1985; Crane et al. 1993; Lauer et al. 1995). The central surface brightness profiles can be parameterized by a single power law in galaxies where no core is resolved (power-law galaxies), while others require a double power law such that the slope within the resolved core is much shallower than the outer slope (core galaxies). According to the widely adopted criteria of Lauer et al. (1995) and Faber et al. (1997), the central surface brightness cusps can be described by  $I(r) \propto r^{-\gamma}$ , with  $\gamma \leq 0.3$  for core galaxies and  $\gamma \geq 0.5$  for power-law galaxies.

Interestingly, this classification based on the cusp slope reflects a distinct dichotomy in the global photometric and kinematic properties among early-type galaxies. Core galaxies are luminous ( $M_V \lesssim -21$  mag) and have high velocity dispersions, compared to power-law galaxies which have lower luminosities and lower velocity dispersions. Core galaxies have boxy or pure elliptical isophotes and show slow rotation, while power-law galaxies tend to have disk-like isophotes and are fast rotators (Carollo et al. 1997; Faber et al. 1997; Ravindranath et al. 2001b; Rest et al. 2001). Differences between the two classes can also be seen in their X-ray properties (Pellegrini 1999). Thus, it appears that the origin of the inner cusps is closely linked to the formation and subsequent evolution of these galaxies.

Several models with and without central, massive black holes (BHs) have been proposed to explain the formation of cusps and the observed core properties. In models without BHs the cusp slope reflects the amount of dissipation that occurred during the formation process. Steep density cusps seen in low-luminosity elliptical galaxies can result from dissipative, gas-rich mergers (Faber et al. 1997). Numerical simulations of gas-rich mergers have shown that angular momentum transfer can lead to gas inflows, trigger starbursts, and result in the formation of dense

cores (e.g., Barnes & Hernquist 1991). Moreover, even a small amount of gas can cause the isophotes to become disk-like and induce the higher rotation velocities seen in power-law galaxies (Barnes & Hernquist 1996; Kormendy & Bender 1996; Faber et al. 1997). An analogous explanation for the weak cusps seen in luminous ellipticals involves dissipationless, gas-poor mergers (Bender, Burstein, & Faber 1992). Although such models succeed in producing the weaker cusps seen in these objects, the core sizes tend to decrease or remain unchanged in the merger remnant (Farouki, Shapiro, & Duncan 1983; Barnes 1992). In fact, with the increased merger events that would be needed to form giant ellipticals, the cores become denser and more compact, in clear conflict with the empirical trend that giant ellipticals tend to have large-sized, diffuse cores. Even in the case of accretion of a low-mass secondary galaxy by a massive primary galaxy, the dense core of the secondary survives the merger event, thereby resulting in a remnant that has high central density (Holley-Bockelmann & Richstone 1999, 2000; Merritt & Cruz 2001). Thus, models that aim to account for the formation of central density cusps without invoking BHs invariably produce cusps that are steeper than observed and fail to reproduce the scaling relations between galaxy luminosity and core size.

On the other hand, numerical simulations that include the effects of central BHs have proved to be more promising in reproducing the low-density cores seen in luminous ellipticals (Ebisuzaki, Makino, & Okumura 1991; Makino & Ebisuzaki 1996; Nakano & Makino 1999; Milosavljević & Merritt 2001). Ebisuzaki et al. (1991) showed that the observed correlation between core size and total bulge luminosity can result from mergers of equal-mass galaxies containing central BHs. More recent studies have shown that the formation and subsequent orbital decay of a BH binary can destroy the existing steep cusps of the merging galaxies via the interaction of the binary with surrounding stars. During the initial stages of merging, the BHs sink to the center under the influence of dynamical friction from stars and form a binary. The potential energy released as the binary orbit shrinks can eject stars in its vicinity with high veloc-

<sup>1</sup> The Observatories of the Carnegie Institution of Washington, 813 Santa Barbara St., Pasadena, CA 91101-1292.

<sup>2</sup> Department of Astronomy, University of California, Berkeley, CA 94720-3411.

ities, thereby weakening the initial density cusp and expanding the core (Quinlan & Hernquist 1997; Nakano & Makino 1999; Milosavljević & Merritt 2001). The merger models predict that the core size of the merger remnant would show an almost linear dependence with BH mass (Nakano & Makino 1999). During each merger event the scouring action by the BH binary would eject a total mass of the order of the combined mass of the BHs (Quinlan & Hernquist 1997; Milosavljević & Merritt 2001). In addition to the BH mass, the overall mass deficit depends on the number of merger events, and is larger for the more luminous galaxies. Thus, a steeper-than-linear relation is predicted between the ejected mass and the final BH mass (Milosavljević & Merritt 2001).

An alternative model interprets the central cusps in elliptical galaxies as the result of dynamical effects induced by the adiabatic growth of a central BH in an initially isothermal core (e.g., Young et al. 1978; Lauer et al. 1992; Crane et al. 1993; van der Marel 1999a). The growth of BHs in galaxy centers can occur by accretion of gas from stellar mass loss or other sources. Under the adiabatic assumption this growth is slow compared to the dynamical timescale, such that the phase-space distribution function of the stars remains unchanged. Adiabatic growth in an isothermal core induces a weak density cusp of the form  $\rho \propto r^{-3/2}$ , or slightly steeper for the case of a non-isothermal core (Young 1980; Quinlan, Hernquist, & Sigurdsson 1995). According to these models, the slope of the cusp is determined by the ratio of the BH mass to the mass of the initial core. A steeper cusp would result from a larger fractional BH mass. This is in contrast to the expectations of the merger models, where a more massive BH would cause the cusp to weaken. The cusp slope and the cusp scale length of the surface brightness profiles derived from adiabatic-growth models is found to correlate well with the BH mass (Cipollina & Bertin 1994). Van der Marel (1999a) has shown that the adiabatic models can reproduce the range of inner-cusp slopes and core radii seen in the *HST* images and can be used to predict BH masses.

In this paper, we use a large database of observed central parameters of early-type galaxies to test the viability of the adiabatic BH growth and binary BH merger models. High-resolution surface brightness profiles are currently available for many early-type galaxies. The discovery of a tight correlation between BH mass and bulge velocity dispersion (Gebhardt et al. 2000; Ferrarese & Merritt 2000) allows us to estimate BH masses accurately and efficiently. These recent developments provide an opportunity to test the models. Section 2 describes the sample and the sources from which the data were compiled. We present the observed correlations in § 3 and discuss their implications in § 4. A preliminary version of this work was presented in Ravindranath, Ho, & Filippenko (2001a).

## 2. THE SAMPLE

The sample chosen for the present study comprises early-type galaxies that have been observed using *HST* and for which their central surface brightness profiles (within a radius of  $\sim 10''$ ) have been parameterized in the literature using the “Nuker” function (Lauer et al. 1995). This function has the form

$$I(r) = 2^{(\beta-\gamma)/\alpha} I_b \left( \frac{r}{r_b} \right)^{-\gamma} \left[ 1 + \left( \frac{r}{r_b} \right)^\alpha \right]^{(\gamma-\beta)/\alpha}, \quad (1)$$

where  $\beta$  is the asymptotic slope as  $r \rightarrow \infty$ ,  $\gamma$  is the asymptotic

slope as  $r \rightarrow 0$ ,  $r_b$  is the break radius at which the outer slope  $\beta$  changes to the inner slope  $\gamma$ ,  $\alpha$  controls the sharpness of the transition between the inner and outer slopes, and  $I_b$  is the surface brightness at  $r_b$ .

The sample is derived mainly from three sources. (1) Faber et al. (1997) give Nuker parameters for 58 nearby early-type galaxies that were observed using WFPC in the *V* band. These include galaxies in the Local Group, ellipticals and S0s in the Virgo cluster, and the bulges of a few nearby early-type spiral galaxies. (2) Rest et al. (2001) obtained *R*-band images of 67 early-type galaxies using WFPC2 and fitted Nuker functions to the light profiles of 58 of these. Their sample comprises all early-type galaxies from the Lyon/Meudon Extragalactic Database with radial velocities less than  $3400 \text{ km s}^{-1}$ , absolute *V*-band magnitudes less than  $-18.5$ , and Galactic latitudes greater than  $20^\circ$ . (3) Ravindranath et al. (2001b) used the Nuker function to perform two-dimensional fits of the central regions of 33 early-type galaxies observed with NICMOS in the *H* band. The galaxies were chosen from the Palomar survey of nearby galaxies, a ground-based optical spectroscopic study of a nearly complete sample of 486 galaxies with  $B_T \leq 12.5$  mag and  $\delta > 0^\circ$  (Filippenko & Sargent 1985; Ho, Filippenko & Sargent 1995).

From these sources, we compiled a database consisting of galaxies for which the classification of the central surface brightness profile type is unambiguous. Only galaxies with inner slope  $\gamma \leq 0.3$ , break radius  $r_b > 0''.2$ , and  $\alpha > 0.8$  were included as core galaxies, to ensure that the core region is well resolved. Objects with  $\gamma \geq 0.5$  constitute power-law galaxies in the sample. We did not include in the present analysis the few objects that have intermediate slopes ( $0.3 < \gamma < 0.5$ ). We also excluded galaxies lacking stellar velocity dispersion measurements, which we later use to estimate BH masses (§ 4). The final database consists of 88 sources (38 core galaxies and 50 power-law galaxies), the properties of which are given in Tables 1A and 1B, respectively.

Since the above data were taken in different bands, it is important to verify whether the central parameters vary with wavelength, as would be expected if there are significant differences in the stellar population or dust extinction. Ravindranath et al. (2001b) compared the Nuker parameters derived from optical and near-infrared images. Even though the outer slope  $\beta$  can be significantly different between the two bands (a consequence of radial color gradients), the inner slope  $\gamma$  and the break radius  $r_b$  show good overall agreement. Another concern when using data from various sources is to ensure that physical parameters are derived using the same distance scale. The apparent quantities from the literature were converted to absolute quantities using distances from Tonry et al. (2001), when available, which are based on measurements of *I*-band surface brightness fluctuations. The distances for the remaining galaxies were calculated from the radial velocities given in the Third Reference Catalogue of Bright Galaxies (de Vaucouleurs et al. 1991) using a Hubble constant of  $H_0 = 75 \text{ km s}^{-1} \text{ Mpc}^{-1}$ .

## 3. COMPARISON OF DATA WITH MODEL PREDICTIONS

Both the adiabatic-growth model and the binary BH model attempt to explain the formation of cores and weak cusps in elliptical galaxies based on the dynamical effects of BHs. We compare the relation between the observed quantities (core radius, inner-cusp slope, and BH mass) with the relations predicted from these models. The BH masses required for the anal-

TABLE 1A: PROPERTIES OF CORE GALAXIES IN THE SAMPLE

Galaxy Name	$D$ (Mpc)	$\sigma_0$ (km s <sup>-1</sup> )	$\log r_e$	$\log r_b$	$\gamma$	$\gamma'$	Reference
(1)	(2)	(3)	(4)	(5)	(6)	(7)	(8)
A 1020	260.0	345	...	2.480	0.17	1.07	1
A 2052	140.8	247	...	2.457	0.20	1.19	1
NGC 524	23.9	245	3.590	2.214	0.03	0.72	2
NGC 720	27.6	237	3.723	2.634	0.06	1.03	1
NGC 1052	19.4	215	3.540	1.575	0.11	0.92	2
NGC 1316	21.4	250	3.923	1.630	0.00	0.16	1
NGC 1399	19.9	359	3.611	2.482	0.07	1.01	1
NGC 1400	26.4	261	3.684	1.626	0.00	0.09	1
NGC 1600	62.5	333	4.158	2.975	0.08	1.05	1
NGC 2832	92.6	328	2.139	2.611	0.02	0.74	1
NGC 2986	30.7	268	3.789	2.265	0.18	1.15	3
NGC 3348	37.8	237	3.670	2.258	0.09	0.95	3
NGC 3379	10.5	221	3.253	1.908	0.18	1.16	2
NGC 3608	22.9	195	3.592	1.492	0.00	0.28	1
NGC 3613	29.1	213	3.536	1.680	0.04	0.73	3
NGC 3640	27.0	184	3.634	1.761	0.15	1.03	3
NGC 4168	30.4	186	3.826	2.570	0.14	1.07	1
NGC 4261	31.6	309	3.772	2.395	0.00	0.00	2
NGC 4278	16.0	251	3.406	1.878	0.02	0.69	2
NGC 4291	26.1	284	3.269	1.784	0.02	0.58	2
NGC 4365	20.4	269	3.752	2.218	0.15	1.13	1
NGC 4374	18.3	293	3.685	2.327	0.13	1.12	2
NGC 4406	17.1	246	3.875	1.919	0.00	0.00	2
NGC 4472	16.3	303	3.914	2.317	0.04	0.95	2
NGC 4486	16.0	339	3.906	2.772	0.25	1.25	1
NGC 4552	15.3	263	3.347	1.684	0.00	0.03	1
NGC 4589	21.9	225	3.643	1.349	0.11	0.90	2
NGC 4636	14.6	209	3.854	2.388	0.13	1.12	2
NGC 4649	16.8	343	3.778	2.465	0.15	1.14	1
NGC 4874	96.3	266	4.456	3.089	0.13	1.12	1
NGC 4889	86.5	381	4.120	2.848	0.05	0.99	1
NGC 5077	37.5	260	3.657	2.467	0.23	1.19	3
NGC 5557	42.8	253	3.774	2.400	0.14	1.02	3
NGC 5813	32.2	230	3.880	2.091	0.08	0.99	1
NGC 5903	33.9	210	3.762	2.417	0.13	1.10	3
NGC 5982	40.2	250	3.686	1.954	0.06	0.85	2
NGC 6166	121.3	302	4.526	3.115	0.08	1.06	1
NGC 7768	109.2	286	4.200	2.325	0.00	0.00	1

NOTE.— Col. (1) Galaxy name. Col. (2) Surface brightness fluctuations distance from Tonry et al. 2001, when available, and otherwise derived from the heliocentric radial velocity and  $H_0 = 75$  km s<sup>-1</sup> Mpc<sup>-1</sup>. Col. (3) Central stellar velocity dispersion from Prugniel & Simien 1996. Col. (4) Logarithm of the effective radius in pc. Col. (5) Logarithm of the break radius in pc. Col. (6) Inner cusp slope of the surface brightness profile. Col. (7) Inner cusp slope of the deprojected luminosity density profile. Col. (8) Reference for  $\gamma$  and  $r_b$ .

REFERENCES.— (1) Faber et al. 1997; (2) Ravindranath et al. 2001b; (3) Rest et al. 2001.

ysis presented here are derived using the empirical correlation between BH mass and bulge stellar velocity dispersion (Gebhardt et al. 2000; Ferrarese & Merritt 2000). Gebhardt et al. (2000) use  $\sigma = \sigma_e$ , the projected, luminosity-weighted velocity dispersion measured within the effective radius  $r_e$ .

For our sample we do not have uniform measurements of  $\sigma_e$ , we use instead  $\sigma = \sigma_0$ , the central velocity dispersion, since in general  $\sigma_e \approx \sigma_0$  within a scatter of  $\sim 10\%$  (Gebhardt et al. 2000). The central velocity dispersions were taken from the compilation by Prugniel & Simien (1996).

### 3.1. Cusp Slopes and Black Hole Masses

The adiabatic-growth model predicts that more massive BHs (relative to galaxy core mass) produce steeper density cusps. This is well illustrated when the inner-cusp slope ( $\gamma$  as parameterized in the Nuker function) is plotted against the dimensionless BH mass  $\mu \equiv M_{\text{BH}}/M_{\text{core}}$  (Cipollina & Bertin 1994; van der Marel 1999a), where  $M_{\text{core}}$  is the mass of the initial isothermal core. We do not have an independent estimate of  $M_{\text{core}}$ , since the observed core properties, by assumption, have been altered by the BH. However, if the initial state of the galaxy can be approximated by an isothermal sphere (as is done in the adiabatic models), the initial core radius would be a fixed fraction of the initial half-mass radius. Since the

TABLE 1B: PROPERTIES OF POWER-LAW GALAXIES IN THE SAMPLE

Galaxy Name	$D$ (Mpc)	$\sigma_0$ (km s <sup>-1</sup> )	$\log r_e$	$\gamma$	$\gamma'$	Reference
(1)	(2)	(3)	(4)	(5)	(6)	(7)
NGC 221	0.8	77	2.175	0.50	1.50	2
NGC 596	21.7	164	3.499	0.55	1.55	1
NGC 821	24.1	209	3.724	0.64	1.64	2
NGC 1023	11.4	212	2.611	0.78	1.78	1
NGC 1172	21.4	117	3.603	1.01	2.01	1
NGC 1426	24.0	153	3.482	0.85	1.85	1
NGC 2549	12.6	154	2.794	0.67	1.67	3
NGC 2592	25.7	282	...	0.92	1.92	3
NGC 2634	33.4	171	3.646	0.81	1.81	3
NGC 2685	11.7	103	2.955	0.73	1.73	2
NGC 2699	26.9	131	...	0.84	1.84	3
NGC 2778	22.9	166	3.262	0.94	1.94	3
NGC 2872	43.2	271	3.638	1.01	2.01	3
NGC 2950	14.9	182	...	0.82	1.82	3
NGC 3065	26.6	164	...	0.79	1.79	3
NGC 3078	35.1	237	3.608	0.95	1.95	3
NGC 3115	9.6	274	3.224	0.73	1.73	2
NGC 3384	11.5	164	2.860	0.64	1.64	2
NGC 3414	25.2	250	2.262	0.83	1.83	3
NGC 3599	20.3	79	3.470	0.79	1.79	1
NGC 3605	20.7	100	3.238	0.67	1.67	1
NGC 3900	23.9	115	3.759	0.51	1.78	2
NGC 4026	13.6	197	2.584	0.51	1.71	2
NGC 4121	29.3	118	2.829	0.85	1.85	3
NGC 4128	31.0	206	...	0.71	1.71	3
NGC 4143	15.9	270	1.790	0.59	1.59	2
NGC 4150	13.7	123	1.725	0.64	1.64	2
NGC 4239	12.5	63	2.989	0.65	1.65	1
NGC 4387	21.3	112	3.201	0.72	1.72	1
NGC 4417	11.2	82	2.134	0.71	1.71	2
NGC 4434	26.8	122	3.380	0.70	1.70	1
NGC 4464	16.5	129	2.632	0.88	1.88	1
NGC 4467	19.0	81	2.951	0.98	1.98	1
NGC 4503	17.9	115	...	0.64	1.64	3
NGC 4551	17.3	114	3.170	0.80	1.80	1
NGC 4570	23.3	190	2.132	0.85	1.85	1
NGC 4621	18.2	237	3.612	0.50	1.76	1
NGC 4648	19.6	222	3.166	0.92	1.92	3
NGC 4697	11.7	174	3.630	0.74	1.74	1
NGC 4742	15.5	102	2.943	1.09	2.09	1
NGC 5017	33.9	174	3.122	1.12	2.12	3
NGC 5308	27.2	230	...	0.82	1.87	3
NGC 5370	40.7	133	...	0.62	1.62	3
NGC 5812	26.9	213	3.492	0.59	1.59	1
NGC 5838	18.1	290	3.237	0.93	1.93	2
NGC 5845	25.9	241	2.705	0.51	1.50	1
NGC 6278	37.2	157	...	0.55	1.55	3
NGC 6340	15.9	147	2.380	0.59	1.58	2
NGC 7332	23.0	136	2.251	0.90	1.90	1
NGC 7743	20.7	84	3.321	0.50	1.48	2

NOTE.— Col. (1) Galaxy name. Col. (2) Surface brightness fluctuations distance from Tonry et al. 2001, when available, and otherwise derived from the heliocentric radial velocity and  $H_0 = 75 \text{ km s}^{-1} \text{ Mpc}^{-1}$ . Col. (3) Central stellar velocity dispersion from Prugniel & Simien 1996. Col. (4) Logarithm of the effective radius in pc. Col. (5) Inner cusp slope of the surface brightness profile. Col. (6) Inner cusp slope of the deprojected luminosity density profile. Col. (7) Reference for  $\gamma$  and  $r_b$ .

REFERENCES.— (1) Faber et al. 1997; (2) Ravindranath et al. 2001b; (3) Rest et al. 2001.

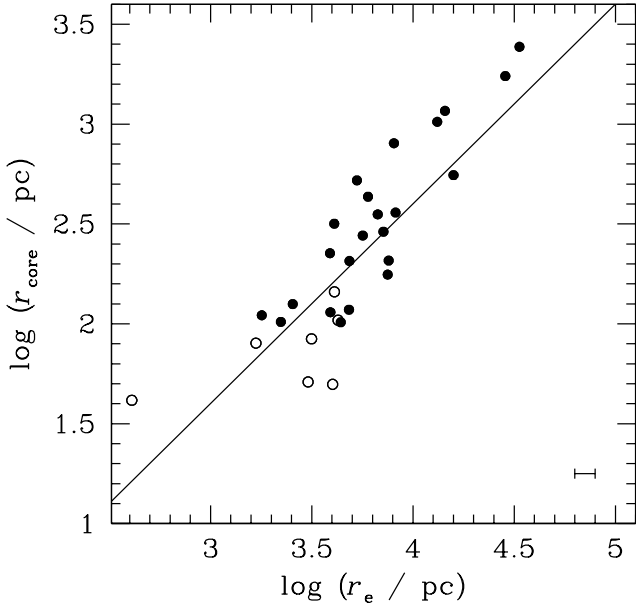


FIG. 1.— The radius of the initial isothermal core for the best-fitting adiabatic-growth model versus the effective radius. Core galaxies are shown as solid points and power-law galaxies as open circles. The solid line has a slope of unity and corresponds to  $r_{\text{core}} = 0.04 r_e$ . Only galaxies common to this study and that of van der Marel (1999a) are shown. A representative error bar for  $r_e$  is given in the lower-right corner of the plot.

adiabatic growth of the BH should not significantly alter the mass distribution at large radii, it is safe to assume that the half-mass radius, or a closely related measure such as the effective radius, remains unaffected. In Figure 1, we plot the core radius from the best-fitting adiabatic model of van der Marel (1999a) versus the effective radius for all galaxies common to both studies. The radius of the isothermal core indeed is well correlated with  $r_e$  and can be approximated as  $r_{\text{core}} \approx 0.04 r_e$ ; the mean scatter about this relation is 0.23 dex. Thus, analogous to  $\mu$ , we define the dimensionless mass  $\mu' \equiv M_{\text{BH}}/M_e$ , where  $M_e$  is the mass within  $r_e$  calculated using  $M_e = 3\sigma^2 r_e / G$ . The effective radii were taken from Faber et al. (1989), Bender et al. (1992), and Baggett, Baggett, & Anderson (1998).

A plot of the observed inner-cusp slope  $\gamma$  versus  $\mu'$  (Fig. 2) does not appear to be consistent with the expectation from the adiabatic-growth model. We have overplotted the theoretical relation between  $\gamma$  and  $\mu$ , as given by Cipollina & Bertin (1994), but shifted arbitrarily in the horizontal direction to allow for a constant scaling between  $\mu$  and  $\mu'$  (i.e., between  $M_{\text{core}}$  and  $M_e$ ). The predicted line matches the data poorly. The largest discrepancy lies with the power-law galaxies, which, because of their steep cusps, are required to have values of  $\mu'$  up to 1–2 orders of magnitude larger than observed. Except for a larger spread, most power-law galaxies, in fact, are characterized by values of  $\mu'$  within the fairly restricted range found in core galaxies ( $\log \mu' \approx -2.9 \pm 0.5$ ). In other words, the BH mass constitutes a roughly constant fraction of the central stellar mass within  $r_e$ , albeit with substantial scatter. This is just the familiar linear correlation between BH mass and bulge mass (Kormendy & Richstone 1995; Magorrian et al. 1998; van der Marel 1999b; Ho 1999; Kormendy & Gebhardt 2001). The distribution of points for the core galaxies might be marginally consistent with the model, but the scatter is large.

Since  $M_e$  is distance dependent, this test may be affected, at least in part, by uncertainties in the distances used. The parameter  $\gamma$  itself is also vulnerable to distance effects because the

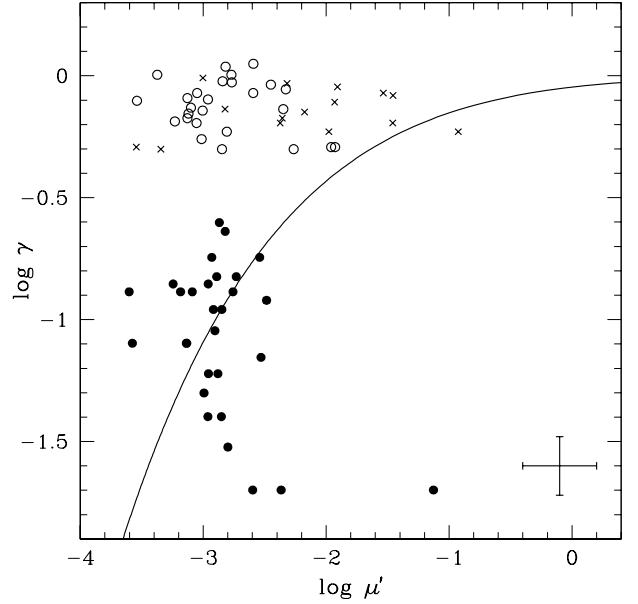


FIG. 2.— The inner-cusp slope  $\gamma$  versus the dimensionless BH mass defined as  $\mu' \equiv M_{\text{BH}}/M_e$ , where  $M_e$  is the total mass within the effective radius. Core galaxies are shown as solid points and power-law galaxies as open circles. Crosses denote galaxies for which the effective radii were derived from bulge-disk decomposition (from Baggett et al. 1998). Representative error bars are given in the lower-right corner of the plot. The solid line gives the theoretical prediction from Cipollina & Bertin (1994) for the relation between  $\gamma$  and  $\mu \equiv M_{\text{BH}}/M_{\text{core}}$ , shifted arbitrarily along the horizontal axis to allow for a constant scaling between  $\mu$  and  $\mu'$ .

cores of distant galaxies may not be sufficiently well resolved to yield the asymptotic inner slope of the Nuker function. This latter effect, however, cannot be strong for the core galaxies in our sample because we have explicitly chosen objects with well-resolved break radii (see § 2). We do not believe that distance errors could have erased an intrinsic trend in Figure 2. The nominal error bars shown on the lower-right corner of the plot are significantly smaller than the observed spread in the data points.

Figure 3a compares the BH masses inferred from adiabatic models by van der Marel (1999a) with independent, direct measurements obtained from stellar and gaseous kinematics (as summarized in Kormendy & Gebhardt 2001); a similar comparison is made in Figure 3b for a larger sample with independent masses derived using the  $M_{\text{BH}} - \sigma$  relation of Gebhardt et al. (2000). The adiabatic models tend to yield masses that are systematically larger, on average by  $\sim 0.5$  dex; the offset is slightly larger for power-law galaxies than core galaxies.

### 3.2. Core Properties and Black Hole Binaries

Simulations of merging galaxies with central BHs produce merger remnants whose core properties correlate well with the final BH mass (Ebisuzaki et al. 1991; Nakano & Makino 1999; Milosavljević & Merritt 2001). Nakano & Makino (1999) studied the dynamical reaction of the central regions of a galaxy, modeled as an isothermal core, to the infall of a massive BH. They found that larger BHs tend to create larger and more massive cores. Figure 4a shows the relation between the observed core size — here represented by the break radius  $r_b$  — and the BH mass. Albeit with substantial scatter, the observed trend qualitatively agrees with the simulations in that more massive BHs produce larger cores. The correlation revealed by our sample is highly statistically significant: the Spearman's  $\rho$

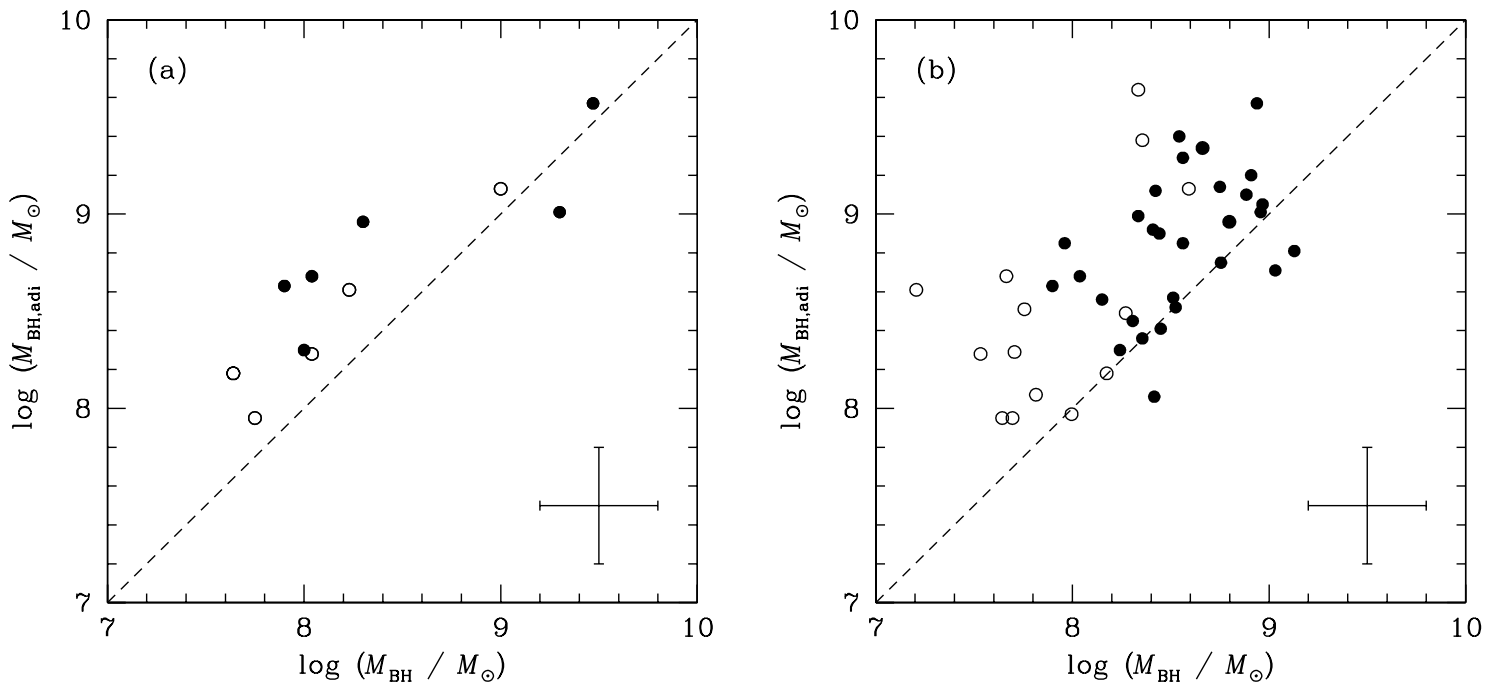


FIG. 3.— Comparison of BH masses obtained from the adiabatic-growth models of van der Marel (1999a) with (a) BH masses derived directly using stellar and gas kinematics (Kormendy & Gebhardt 2001) and (b) BH masses derived using the  $M_{\text{BH}}-\sigma$  relation from Gebhardt et al. (2000). The solid points correspond to core galaxies and open circles to power-law galaxies. Representative error bars are given in the lower-right corner of the plot.

correlation coefficient is 0.57, with a probability of  $5 \times 10^{-4}$  that the two variables are uncorrelated. However, the observed slope is substantially steeper than the unity slope suggested by Nakano & Makino (1999). The best-fitting linear regression line, obtained by adopting  $M_{\text{BH}}$  as the independent variable and including nominal errors on both variables, has a slope of  $\sim 2.8 \pm 0.84$ . It would be fruitful in the future to reexamine this issue using simulations that incorporate more realistic initial conditions.

According to the merger models, more luminous galaxies should have experienced a larger number of mergers than fainter galaxies, and hence their centers should have been “scoured” more thoroughly by the orbital decay of BH binaries. This scenario provides an attractive explanation for the observed correlation between core size and total bulge luminosity (Faber et al. 1997; Ravindranath et al. 2001b). Recently, Milosavljević & Merritt (2001) carried out more realistic simulations that start with galaxies containing central BHs and steep density cusps ( $\rho \propto r^{-2}$ ), as observed in power-law galaxies. Unlike earlier simulations where the dynamical effects of the massive BH were studied by introducing a naked BH into an existing core, their model includes the effect of stars bound to the BHs. This is found to reduce the timescale over which the two BHs approach each other due to dynamical friction and form a binary. As the binary orbit shrinks, the gravitational slingshot effect ejects stars from the center and causes the density cusp to flatten to  $\rho \sim r^{-\gamma'}$ , where  $\gamma' < 2$ . Assuming that the initial central density profiles are represented by steep  $\rho \sim r^{-2}$  cusps, the ejected mass or the mass deficit is defined as the mass needed to recover the initial profile from the observed flat profile with slope  $\gamma'$ . A key prediction from the simulations by Milosavljević & Merritt (2001) is that the mass ejected during each merger event by the BH binary should be comparable to their combined mass. The total mass ejected depends on the final BH mass and

the number of mergers, and hence a steeper-than-linear relation is expected between the mass deficit and BH mass. Milosavljević & Merritt (2001) give the following expression for the ejected mass:

$$M_{\text{ej}} \approx \frac{2(2-\gamma')}{3-\gamma'} \frac{\sigma^2 r_b}{G}, \quad (2)$$

where  $r_b$  is the core radius (equivalent to the break radius in the Nuker function) and  $\gamma'$  is the inner-cusp slope of the luminosity density profile. We obtained the luminosity density profile by inverting the surface brightness profile, parameterized by the Nuker function, using the Abel integral equation and assuming spherical symmetry (Binney & Tremaine 1987). A plot of  $M_{\text{ej}}$  versus  $M_{\text{BH}}$  (Fig. 4b) shows that the two quantities are indeed well correlated. The best-fitting linear regression line, again obtained by adopting  $M_{\text{BH}}$  as the independent variable and including nominal errors on both variables, gives a slope of  $\sim 2.3 \pm 0.51$ . Milosavljević & Merritt (2001) presented a similar result based on a smaller sample. Formally, the correlation in our sample again is statistically very significant; the Spearman’s  $\rho$  correlation coefficient is 0.77, and the probability that the correlation could have arisen by chance is  $< 10^{-4}$ .

We stress that the tightness of the  $M_{\text{BH}}-\sigma$  relation (Gebhardt et al. 2000; Ferrarese & Merritt 2000) implies that there should be little difference between BH masses estimated in this fashion compared to directly measured masses. We illustrate this point in Figure 4 by reploting in open symbols the six objects having kinematically determined BH masses.

#### 4. DISCUSSION AND SUMMARY

As discussed by Faber et al. (1997) and Ravindranath et al. (2001b), the cores of luminous elliptical galaxies populate a core “fundamental plane” (defined by  $r_b$ , surface brightness  $\mu_b$

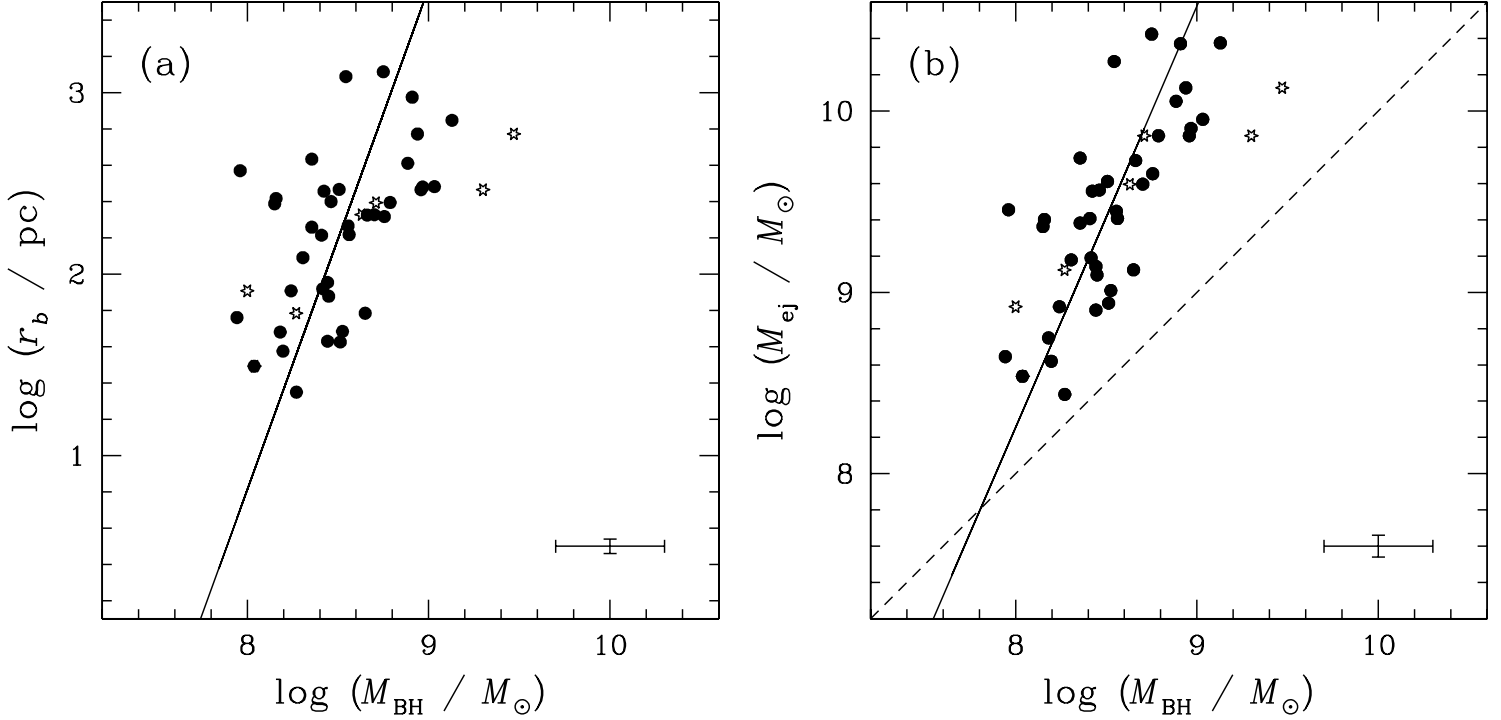


FIG. 4.— The relation among core galaxies between BH mass  $M_{\text{BH}}$  and (a) the break radius  $r_b$  and (b) the ejected mass  $M_{\text{ej}}$ . The solid line in each panel gives the best-fitting linear regression (see text). The dashed line in panel (b) denotes  $M_{\text{ej}} = M_{\text{BH}}$ . The open star symbols replot the six galaxies whose BH masses have been measured directly by kinematics. They do not show any obvious systematic deviations compared to the solid points. Representative error bars are given in the lower-right corner of the plot.

at  $r_b$ , and  $\sigma_0$ ), analogous to the fundamental plane on global scales (defined by  $r_e$ , the surface brightness  $\mu_e$  at  $r_e$ , and  $\sigma_e$ ). More luminous galaxies with higher central velocity dispersions have characteristically larger, more diffuse cores. Most

theories for the formation of early-type galaxies involve dissipative gas inflows that tend to increase the central density and form steep nuclear cusps. While low-luminosity galaxies with power-law profiles can be explained naturally in this manner, the existence of diffuse cores with weak cusps in massive galaxies poses a serious observational challenge, as discussed by Faber et al. (1997). How did they form? And once created, how did they manage to avoid acquiring high-density cores from the accretion of low-mass satellites?

A promising framework to address the formation of cores invokes the dynamical effects of merging central massive BHs. This is all the more appealing because there is now increasing evidence that BHs are ubiquitous in bulges (Magorrian et al. 1998; Ho 1999; Kormendy & Gebhardt 2001). If so, the hierarchical assembly of massive elliptical galaxies would inevitably lead to BH mergers. The most recent simulations by Milosavljević & Merritt (2001) incorporate realistic initial conditions for the merging galaxies. Starting with two low-mass galaxies, each containing a central BH and a steep nuclear cusp, the hardening of the BH binary leads to the formation of a remnant with a large, diffuse core. We show in this paper that galaxy cores obey certain trends that are expected for the merger remnants of binary BHs.

If cores form as an aftermath of galaxy mergers containing BHs, the work of Nakano & Makino (1999) indicates that the sizes of the cores should scale with the final BH mass. Using the  $M_{\text{BH}} - \sigma$  relation to estimate BH mass, we find that this

indeed seems to hold in our sample: the core size increases roughly as  $r_b \propto M_{\text{BH}}^{2.8}$  (Fig. 4a). Although the slope of the correlation is steeper than predicted by Nakano & Makino (1999), the discrepancy should not be taken too literally given the simplified initial conditions used in their numerical calculations. Combining this functional dependence with  $M_{\text{BH}} \propto \sigma^{3.8}$  (Gebhardt et al. 2000), we recover within the errors, the empirical scaling relation between core size and velocity dispersion,  $r_b \propto \sigma^6$  (Faber et al. 1997; Ravindranath et al. 2001b). Thus, in this interpretation, the scaling relation observed between  $r_b$  and  $\sigma$  is an indirect manifestation of two more fundamental correlations, namely the  $r_b - M_{\text{BH}}$  relation which reflects the dynamical effects of binary BHs during core formation, and the  $M_{\text{BH}} - \sigma$  relation which bears on processes associated with the joint formation of BHs and bulges (e.g., Kauffmann & Haehnelt 2000; Burkert & Silk 2001).

Using the numerical models of Quinlan & Hernquist (1997), Faber et al. (1997) already demonstrated that BH mergers produce cores whose masses scale approximately with the final BH mass. They suggested that the relation between core and BH mass might depend on the slope of the nuclear cusp and pointed out the need for simulations with more realistic initial conditions. The calculations of Milosavljević & Merritt (2001) add a new degree of realism to the simulations by modeling the merging galaxies as systems with initially steep cusps, as seen in power-law galaxies. Adopting their formalism to compute the amount of stellar mass ejected by the BH binary during core formation, and again the  $M_{\text{BH}} - \sigma$  relation to estimate BH mass, we find that  $M_{\text{ej}} \propto M_{\text{BH}}^{2.3}$  (Fig. 4b). Unlike the case of the relation between  $r_b$  and  $M_{\text{BH}}$ , the slope of the correlation between  $M_{\text{ej}}$  and  $M_{\text{BH}}$  cannot be easily traced to known central-parameter scaling relations. The  $r_b - \sigma$  and  $M_{\text{BH}} - \sigma$  relations,

when combined with Equation 2, yields a slope of  $\sim 4$  for the  $M_{\text{ej}} - M_{\text{BH}}$  relation, whereas the actual observed slope is  $\sim 2$ . Although each merger produces  $M_{\text{ej}} \approx M_{\text{BH}}$ , the total ejected mass depends on the number of mergers; more massive galaxies with more massive BHs require a larger number of mergers, and thus the slope of the  $M_{\text{ej}} - M_{\text{BH}}$  is expected to be  $> 1$ . This is in qualitative agreement with the observations. In detail, of course, the exact slope should depend on complications not treated in the models. These include heterogeneous mergers and additional processes such as gas accretion.

A competing view of core formation posits that the nuclear cusps imprint the formation of the central BH through adiabatic growth. According to this picture, the slope of the cusp profile should correlate with the relative BH mass fraction; for a galaxy core of a given mass, a more massive BH induces a steeper cusp. This basic expectation, however, is not supported by the data. The strongest disagreement comes from the power-law galaxies, whose steep cusps would suggest that these objects have exceptionally large BH mass fractions, contrary to what is actually observed. The core galaxies fare somewhat better. The distribution of cusp slopes versus BH mass fraction is not inconsistent with the sharp rise anticipated by the models (Fig. 2), although the agreement cannot be said to be good. Regardless of this comparison, however, a basic shortcoming of the adiabatic-growth model is that it leaves the main problem of the formation of cores unanswered; the BH is assumed to grow in a preexisting core.

As shown by van der Marel (1999a), one of the most attractive features of the adiabatic model is that it potentially allows us to estimate BH masses based on photometric data alone. This would be a remarkably efficient alternative to the time-consuming spectroscopic observations needed for the conventional methods based on kinematics. In view of the difficulties described above, it might come as a surprise that the BH masses derived from the adiabatic models should differ from the actual masses by just  $\sim 0.5$  dex (Fig. 3). This is not entirely un-

expected, however, given that the adiabatic models were fitted specifically to the core region of the central light profiles, whose size,  $r_b$  (see Table 1A), is typically only a factor of a few larger than the “sphere of influence” of the BH,  $r_{\text{BH}} \simeq GM_{\text{BH}}/\sigma^2$ . In other words, the mass scale of the initial core, set by the core size, is comparable to the BH mass. In § 3.1, we noted that the offset between the model-inferred masses and the actual masses tends to be systematically larger for power-law galaxies than it is for core galaxies (Fig. 3). This is a simple consequence of the fact that the adiabatic models need to invoke larger BH mass fractions ( $\mu$ ) to fit power-law galaxies than in core galaxies, whereas empirically both types of galaxies share rather similar BH mass fractions.

In summary, we find that the existing data on the central regions of early-type galaxies support the notion that the observed properties of the cores in luminous galaxies have been substantially molded by the dynamical influence of binary massive BHs during past merger events. The merger hypothesis can consistently account for the core fundamental-plane relations and the dependence of core size and mass on central BH mass. The observed cusp slopes do not appear to comply with the expectations of the adiabatic-growth model for BHs.

This work is funded by NASA LTSA grant NAG 5-3556, and by NASA/HST grants AR-07527 and AR-08361 from the Space Telescope Science Institute (operated by AURA, Inc., under NASA contract NAS5-26555). A. V. F. is grateful to the Guggenheim Foundation for a Fellowship. We thank Chien Y. Peng for writing the program to compute the luminosity density profiles, Roeland P. van der Marel for helpful discussions on the adiabatic-growth models, and the referee for constructive criticisms. We made use of the NASA/IPAC Extragalactic Database (NED) which is operated by the Jet Propulsion Laboratory, California Institute of Technology, under contract with NASA, and of the Lyon-Meudon Extragalactic Database.

## REFERENCES

- Baggett, W. E., Baggett, S. M., & Anderson, K. S. J. 1998, *AJ*, 116, 1626  
 Barnes, J. E. 1992, *ApJ*, 393, 484  
 Barnes, J. E., & Hernquist, L. 1991, *ApJ*, 370, L65  
 ——. 1996, *ApJ*, 471, 115  
 Bender, R., Burstein, D., & Faber, S. M. 1992, *AJ*, 399, 462  
 Binney, J., & Tremaine, S. 1987, *Galactic Dynamics* (Princeton: Princeton Univ. Press)  
 Burkert, A., & Silk, J. 2001, *ApJ*, 554, L151  
 Carollo, C. M., Franx, M., Illingworth, G. D., & Forbes, D. A. 1997, *ApJ*, 481, 710  
 Cipollina, M., & Bertin, G. 1994, *A&A*, 288, 43  
 Crane, P., et al. 1993, *AJ*, 106, 1371  
 de Vaucouleurs, G., de Vaucouleurs, A., Corwin, H. G., Jr., Buta, R. J., Paturel, G., & Fouqué, R. 1991, *Third Reference Catalogue of Bright Galaxies* (New York: Springer)  
 Ebisuzaki, T., Makino, J., & Okumura, S. K. 1991, *Nature*, 354, 212  
 Faber, S. M., et al. 1997, *AJ*, 114, 1771  
 Faber, S. M., Wegner, G., Burstein, D., Davies, R. L., Dressler, A., Lynden-Bell, D., & Terlevich, R. J. 1989, *ApJS*, 69, 763  
 Farouki, R. T., Shapiro, S. L., & Duncan, M. J. 1983, *ApJ*, 265, 597  
 Ferrarese, L., & Merritt, D. 2000, *ApJ*, 539, L9  
 Filippenko, A. V., & Sargent, W. L. W. 1985, *ApJS*, 57, 503  
 Gebhardt, K., et al. 2000, *ApJ*, 539, L13  
 Ho, L. C. 1999, in *Observational Evidence for Black Holes in the Universe*, ed. S. K. Chakrabarti (Dordrecht: Kluwer), 157  
 Ho, L. C., Filippenko, A. V., & Sargent, W. L. W. 1995, *ApJS*, 98, 477  
 Holley-Bockelmann, K., & Richstone, D. O. 1999, *ApJ*, 517, 92  
 ——. 2000, *ApJ*, 531, 232  
 Kauffmann, G., & Haehnelt, M. 2000, *MNRAS*, 311, 576  
 Kormendy, J. 1985, *ApJ*, 292, L9  
 Kormendy, J., & Bender, R. 1996, *ApJ*, 464, L119  
 Kormendy, J., & Gebhardt, K. 2001, in *The 20th Texas Symposium on Relativistic Astrophysics*, ed. H. Martel & J. C. Wheeler (New York: AIP), in press  
 Kormendy, J., & Richstone, D. O. 1995, *ARA&A*, 33, 581  
 Lauer, T. R. 1985, *ApJ*, 292, 104  
 Lauer, T. R., et al. 1992, *AJ*, 103, 703  
 ——. 1995, *AJ*, 110, 2622  
 Magorrian, J., et al. 1998, *AJ*, 115, 228  
 Makino, J., & Ebisuzaki, T. 1996, *ApJ*, 465, 527  
 Merritt, D., & Cruz, F. 2001, *ApJ*, 551, L41  
 Milosavljević, M., & Merritt, D. 2001, *ApJ*, in press  
 Nakano, T., & Makino, J. 1999, *ApJ*, 510, 155  
 Pellegrini, S. 1999, *A&A*, 351, 487  
 Prugniel, Ph., & Simien, F. 1996, *A&A*, 309, 749  
 Quinlan, G. D., & Hernquist, L. 1997, *NewA*, 2, 533  
 Quinlan, G. D., Hernquist, L., & Sigurdsson, S. 1995, *ApJ*, 440, 554  
 Ravindranath, S., Ho, L. C., & Filippenko, A. V. 2001a, *BAAS*, 198, 93.02  
 Ravindranath, S., Ho, L. C., Peng, C. Y., Filippenko, A. V., & Sargent, W. L. W. 2001b, *AJ*, 122, 653  
 Rest, A., van den Bosch, F. C., Jaffe, W., Tran, H., Tsvetanov, Z., Ford, H. C., Davies, J., & Schafer, J. 2001, *AJ*, 121, 2431  
 Richstone, D. O., et al. 1998, *Nature*, 395, A14  
 Tonry, J., Dressler, A., Blakeslee, J. P., Ajhar, E. A., Fletcher, A. B., Luppino, G. A., Metzger, M. R., & Moore, C. B. 2001, *ApJ*, 546, 681  
 van der Marel, R. P. 1999a, *AJ*, 117, 744  
 ——. 1999b, in *IAU Symp. 186, Galaxy Interactions at Low and High Redshift*, ed. J. E. Barnes & D. B. Sanders (Dordrecht: Kluwer), 333  
 Young, P. J. 1980, *ApJ*, 242, 1232  
 Young, P. J., Westphal, J. A., Kristian, J., Wilson, C. P., & Landauer, F. P. 1978, *ApJ*, 221, 721